Spatial Dynamics Lab

School of Architecture Planning and Environmental Policy

University College Dublin

Implementation and Analysis of an Experimental Green Roof System with Runoff Reduction Modeling

PI of the project

Professor Francesco Pilla

April 2024

Contents

Abstract

Green roofs (GRs) play a significant role in urban greening and climate adaptation, particularly in densely populated areas. Assessing the effectiveness of GR systems by analyzing runoff reduction parameters is crucial for their design and implementation. The correct version is: "This study, funded by the Climate Action Regional Offices (CARO), went beyond traditional assessments by utilizing advanced sensors to meticulously collect meteorological, rainfall, and runoff data from four green roof installations at locations across Dublin, Ireland. The comprehensive data collected enabled the detailed modeling of runoff hydrograph parameters using rainfall hyetographs, which allowed for a more in-depth analysis of the green roof system's performance. This research focuses on modeling the main runoff characteristic parameters such as Water Retention Amount (WRA), Total Runoff Volume (TRUV), Runoff Peak Flow Maximum (RUPFM), Peak Flow Reduction (PFR), and Runoff Peak Delay to Rainfall Peak (RPDRP). These parameters are essential for understanding how green roof systems can increase water retention and delay rainfall peak times. The findings indicate that the green roof system in our case study retains 75% of rainfall for events that the rainfall volume was less than 1.5 mm per event and, on average, retains 55.69% of rainfall volume. The results also demonstrate that the green roof system is capable of delaying runoff 1.74 hours. Additionally, the system reduces rainfall intensity by 82.78% for events with the rainfall volume up to 1.5 mm per event and by 38% for events exceeding 6 mm per event. Furthermore, the results show a high correlation between runoff characteristics such as WRA and TRUV and rainfall parameters such as Total Rainfall Volume (TRAV) and Rainfall Intensity at Peak (RIP). This correlation suggests that these parameters can be utilized for future modeling to evaluate the efficiency of green roof systems and predict their capability under future climate scenarios.

Keywords: Green roof, Machine Learning, Runoff Hydrograph, Rainfall Hyetographs, Rainfall-Runoff Modeling, Water Retention

1. Introduction

In recent decades, the expansion and development of cities have grown rapidly, leading to the rise of impermeable surfaces, particularly in urban areas (Bhatta, 2010; Firozjaei et al., 2020; OWUSU et al., 2023). Population growth and infrastructure development have led to the replacement of natural permeable covers such as green spaces, agricultural lands, meadows, and wetlands with impermeable surfaces like buildings, pavement, and roads (Firozjaei et al., 2018; Firozjaei et al., 2019; Fu et al., 2019). The increase in impervious surfaces results in a reduction in soil capacity and permeability, leading to decreased infiltration and water storage in the soil (Pappas et al., 2008; Shuster et al., 2005). This gradual decline in soil permeability increases runoff in urban areas and raises the risk of urban flooding (Qin, 2020; Xu et al., 2020; Zhu et al., 2019). Furthermore, concerns have grown about the occurrence of floods due to changes in the frequency, intensity, and duration of extreme weather events, as well as the impacts of global warming in recent years (Bayat-Afshary & Danesh-Yazdi, 2023; Chen et al., 2023; Feyen et al., 2008; Furtak & Wolińska, 2023; Rahmani & Fattahi, 2024; Schreider et al., 2000; Tamm et al., 2023). Therefore, providing solutions to reduce and manage runoff in urban areas has become of paramount importance (Mentens et al., 2006; Shafique et al., 2018). Today, urban managers and planners are focusing on mitigating the negative effects of urban development on microclimate conditions, specifically urban runoff, in order to align with the concept of sustainable development (Getter & Rowe, 2006; Huong & Pathirana, 2013). Nature-Based Solutions (NBS) involve methods to deal with environmental issues by both lessening their impact and adjusting to them. These methods aim to create a balanced connection between living things and their environment by increasing biodiversity, encouraging more green areas, and making cities more sustainable (Cohen-Shacham et al., 2016). In these cities, green technologies such as Best Management Practices (BMP) and Low Impact Development (LID) methods have become popular (Poë et al., 2015; Stovin et al., 2015; Wu et al., 2008). Green roofs, also known as living roofs or eco-roofs, are a type of green technology designed to address environmental challenges. As artificial ecosystems, they offer a nature-based solution (NBS) to issues like climate change and the urban heat island effect. Green roofs can help mitigate urban runoff by managing rainfall at its source, providing beneficial outcomes under specific conditions (Basu et al., 2021; Li et al., 2018; Nawaz et al., 2015; Wong & Jim, 2014). Green roofs involve covering a building with vegetation, which absorbs and retains a portion of rainfall and undergoes processes of evaporation and transpiration, thereby reducing the volume and peak of urban runoff (Metselaar, 2012; Morgan et al., 2013; Roehr & Kong, 2010).

Green roofs are most effective in areas with a higher percentage of rooftop coverage, such as densely urbanized, commercial, and industrial zones (Brandão et al., 2017; Mentens et al., 2006; Roehr & Kong, 2010; Stovin, 2010). Green roofs offer various advantages, including reducing the risk of floods, minimizing the cost of developing and maintaining drainage systems, improving air and water quality, preserving urban beauty, and reducing energy loss from building rooftops (Basu et al., 2021; Palermo et al., 2019). While rainfall characteristics are not controllable, the efficiency of these systems in reducing runoff can be improved by optimizing green roof properties and structure (Liu et al., 2019; Soulis et al., 2017). Numerous studies have evaluated the performance of green roof systems in different cities. Moran (MORAN et al., 2004) conducted a study in North Carolina over a 9-month period to assess the impact of green roofs on runoff quantity and quality. Their findings showed that green roofs in the area could retain approximately 60% of the total rainfall volume and reduce the peak flow rate by around 80%. Mentens (Mentens et al., 2006) concluded that green roofs retain less rainwater in winter compared to summer due to antecedent moisture and evaporation and transpiration. Speak et al. (2013) analyzed 69 rainfall events, identifying October–December as the wettest period (80.7–92.5 mm of rainfall), while February–May is the driest (51.4–61.2 mm of rainfall) in Manchester, UK. Stovin et al. (2012) tested the hydrological performance of a green roof system under the UK climate over a 29-month period from January 1, 2007, to May 31, 2009, identifying July as the driest month and December as the wettest, with an overall retention of 50.2%. Stovin (2010) demonstrated that green roofs can retain stormwater in the British climate and significantly reduce runoff. In this region, green roofs showed an effective reduction of 65-100% in dry seasons, 10-35% in wet seasons, and an average reduction of 34% in all storm events. Hakimdavar (Hakimdavar et al., 2014) found that the depth of rainfall and event duration had the most significant effect on overall green roof rainwater retention. The ability of green roofs to retain water and reduce peak runoff generally decreases with an increase in rainfall volume and duration. Li (Li et al., 2018) showed that the runoff reduction capacity of extensive green roofs can be improved by selecting plant species with higher stem biomass and higher evapotranspiration rates. Palermo (Palermo et al., 2019) conducted a study that showed the range of runoff reduction for green roofs with different soil depths. They found that green roofs with a soil depth of 60 millimeters had a runoff reduction of 22%, while green roofs with a soil depth of 150 millimeters had a runoff reduction of 24%. Interestingly, doubling the soil depth did not significantly increase the reduction in runoff volume. The study

also found that the performance of green roofs in reducing peak flow and other hydrological characteristics was strongly correlated with storm event features in the Mediterranean climate.

As previously noted, existing studies into the efficacy of green roofs on surface runoff have predominantly utilized simulation-based methodologies (Graceson et al., 2013) or traditional statistical analyses (example One-way ANOVA, correlation, etc.) (Mentens et al., 2006; Soulis & Valiantzas, 2012; Speak et al., 2013; Wong & Jim, 2014). These approaches often fail to capture the intricate dynamics of runoff due to their limited ability to consider the complex interplay of various rainfall parameters and weather conditions. To address this gap, this study particularly focuses on data-driven approach, employing advanced machine learning algorithms to delve deeper into nonlinear latent relationships that influence runoff characteristics. This approach not only provides a more nuanced understanding but also enhances the predictive accuracy of runoff parameters from green roofs. The primary innovation of this research lies in its comprehensive analysis of the hydrological performance of green roof systems under various weather condition. By analyzing runoff characteristics through advanced machine learning models, this study significantly influences decision-making processes related to the design and implementation of green roofs. This research will meticulously assess the effects of rainfall characteristics, antecedent moisture conditions, relative humidity, air temperature, and wind speed on the system's performance. A novel contribution of this study is the development of a multivariate model that will predict various runoff characteristics resulting from the green roof system. By integrating machine learning techniques, this research aims to provide actionable insights into optimizing green roof designs for improved environmental and urban resilience.

2. Case studies and green roof sites

We have implemented green roof systems at four distinct locations across Dublin. **Table 1** below provides detailed specifications of these sites, while **Figure 1** shows their mapped locations, with additional information on cradle implementations at each site. The chosen sites are primarily located in southern Dublin, near the confluence of the Dodder and Liffey Rivers. This area is close to the city’s tech district and has high economic value, particularly in the Silicon Docks, where approximately 10% of Ireland’s national income is generated. Given the area's susceptibility to flooding, any disruption could have substantial economic consequences. Therefore, this study’s

goal is to assess the hydrological effectiveness of green roofs in these vulnerable, high-stakes urban environments, providing insights that could inform flood risk management across similar urban areas. (Table1, Figure 1).

The Rosemount site, which covers a longer monitoring period than other sites, was prioritized in the analysis to evaluate the impact of green roofs on runoff reduction. Five green roof cradles were established at this site. The fifth cradle, designed without vegetation, serves as a control, allowing us to measure rainfall effects without plant-based retention. The remaining four cradles, each planted with **Sedum**, provide data on vegetated runoff characteristics (Figure 2). Rainfall at this site was recorded using two methods: (a) an empty cradle for direct rainfall collection, and (b) advanced radar-based Ecomet sensors to capture meteorological parameters such as rainfall intensity, humidity, and wind speed (Figure 3). This setup ensures accurate, site-specific data for modeling runoff dynamics, supporting a detailed comparison between vegetated and non-vegetated setups in subsequent analysis

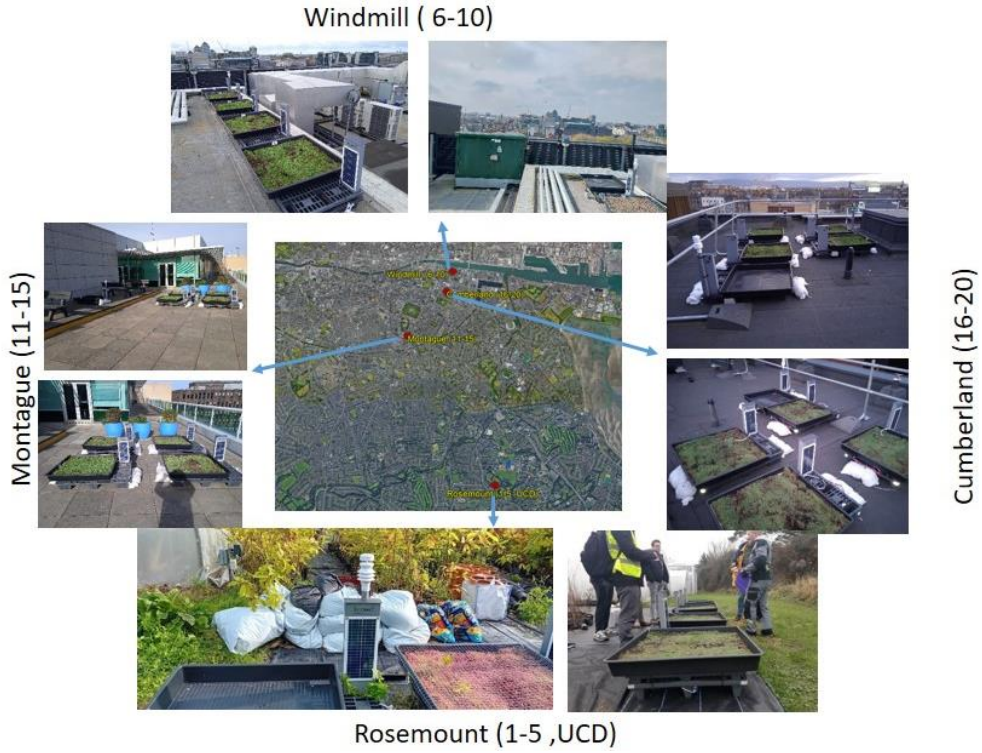

Figure 1. The designed system in four pilots studies for evaluating the efficiency of green roofs in reducing runoff, Dublin city.

Table 1. Green roof sites characteristics

Site names	location	Availability dataset	Cradles number
Rosemount	53.305111°, -6.233078°	2022/12/24	1 to 5
Windmill	53.345691°, -6.246242°	2024/01/03	6 to 10
Montague	53.333024°,-6.260052°	2023/12/15	11 to 15
Cumberland	53.341717°,-6.248226°	2023/12/15	16 to 20

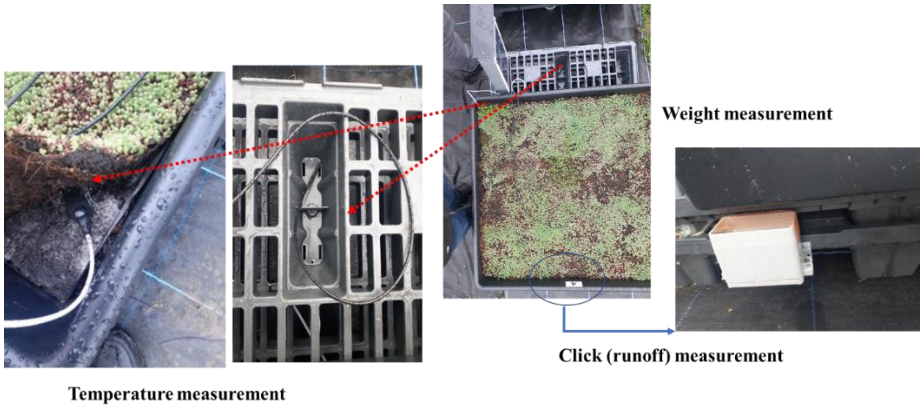

Figure 2. Measurement tools for green roof system, including: dry temperature, surface temperature, subsurface temperature; soil moisture; cradle weight; runoff discharge.

Figure 3. Ecomet tool (mini weather station tool) for metrological parameters measurement, including air temperature, relative humidity, precipitation (radar based), water vapor pressure, air pressure, wind speed and wind direction.

Extensive research has established Sedum as a popular vegetation choice for green roofs, largely due to its drought tolerance, minimal maintenance requirements, and capacity to thrive in shallow soil depths(Graceson et al., 2013; Kemp et al., 2019; Liu et al., 2019; VanWoert et al., 2005; Yang et al., 2015). Sedum's succulence enables it to store water, allowing it to survive variable moisture levels, while its minimal need for watering, fertilizing, or mowing makes it a cost-effective,

practical solution for green roof installations They require minimal maintenance compared to other plant species, as they don't need frequent watering, fertilizing, or mowing, making them a cost-effective and practical choice (Monterusso et al., 2002; VanWoert et al., 2005). Sedum has a shallow root system, well-suited to the thin substrate layers typically used on green roofs, minimizing the weight load on the roof structure while still providing sufficient plant stability and coverage. Additionally, Sedum is a hardy plant that can thrive in harsh conditions, including high winds, intense sunlight, and temperature fluctuations, common in rooftop environments. It spreads quickly, providing rapid ground cover and quickly establishing a green roof, offering benefits such as insulation and stormwater management. Furthermore, the many varieties of Sedum with different colors and textures contribute to the biodiversity and aesthetic appeal of green roofs (Butler et al., 2012).

Sedum species, while popular for green roofs due to their adaptability to shallow soil profiles, have some limitations that might reduce their effectiveness in specific environments. Their shallow roots, for instance, are well-suited to minimal substrate depths but limit their ability to stabilize deeper soil or withstand high winds in exposed rooftop settings (Monterusso et al., 2002). Additionally, certain Sedum varieties are less cold-hardy and may struggle in severe winter climates, potentially requiring replanting or supplementing with more resilient species to maintain year-round coverage (Nagase & Dunnett, 2011). Moreover, Sedum can take longer to establish full coverage compared to other ground covers, delaying soil stabilization and aesthetic benefits on green roofs (Getter & Rowe, 2009). While drought-tolerant, Sedum is vulnerable to fungal diseases and pests in overly humid conditions, potentially necessitating more maintenance in such climates (Snodgrass & Snodgrass, 2006).

2.1 Expert Consultation on Sedum, Soil Material, and Layer Depth

The final selection of Sedum, soil type, and the depth of each layer in the green roof system was a collaborative decision, informed by consultations with green roof experts and environmental scientists (See Table 2). This team carefully considered factors like plant hardiness, local climate, and the project's specific runoff reduction goals. Experts provided input that led to the selection of Sedum over other species, balancing resilience and compatibility with each site's weight load restrictions. In addition, recommendations on soil material and substrate depth helped to optimize

water retention and support the vegetation layer while preserving the structural integrity of the roof systems. Sedum was chosen as the vegetation cover for our green roof design based on its proven durability and minimal maintenance needs, making it well-suited for Dublin's urban climate. Sedum was chosen as the vegetation cover for our green roof design based on its proven durability and minimal maintenance needs, making it well-suited for Dublin's urban climate(Basu et al., 2021). This choice was further supported through consultation with green roof specialists, who advised that Sedum's combination of drought tolerance, lightweight structure, and ease of maintenance aligns with the study's goals and the structural limitations of rooftop installations.

Table 2. Green Roof Layer Depths and Composition

	Minimum Wight (Kg)	**Maximum Wight (Kg)**	**Vegetation type**	**Vegetation depth (cm)**	**Soil/Substrate Layer Depth (cm)**	**Drainage Layer Depth (cm)**	**Geotextile Filter Depth (cm)**	**Waterproof Membrane Depth (cm**
Cradle 1	25	41	Turf	2	2-3	3-5	1-2	1-2
Cradle 2	29	45	Turf	2	2-3	3-5	1-2	1-2
Cradle 3	22	38	Sedum	3	2-3	3-5	1-2	1-2
Cradle 4	23	40	Sedum	3	2-3	3-5	1-2	1-2

Table 2 outlines the depth of each layer, adjusted according to individual site specifications and load-bearing requirements. For instance, Rosemount features a slightly deeper drainage layer to handle the larger expected runoff. Additionally, on April 15, 2024, two cradles at Rosemount were planted with turf in place of Sedum to assess differences in water retention and runoff delay. Including turf enables a comparative analysis of vegetation effects, especially concerning Sedum's performance in retaining water across varying rainfall intensities. A green roof typically comprises five essential layers: (i) the vegetation layer, (ii) the planting substrate (soil), (iii) a geotextile filter, (iv) a drainage layer, and (v) a waterproof membrane to protect the underlying roof. The waterproof layer prevents leakage, facilitating easier repairs, while the drainage layer directs water runoff, preventing waterlogging. The geotextile filter prevents soil particles from entering and clogging the drainage layer, ensuring sustained water flow. Together, the soil and vegetation layers contribute to runoff reduction through processes of evapotranspiration and water storage. The

specific structure and characteristics of each green roof layer influence its effectiveness in runoff management, although the fundamental components remain consistent(Basu et al., 2021). In general, green roof structures include a vegetation layer, growth substrate, filter fabric, drainage component, protection layer, root barrier, insulation layer, waterproofing membrane, and the roof deck (Figure 4). This multi-layered structure was maintained in our green roof sites and cradles to ensure consistent performance and data comparability. The primary variation across green roof cradles at our study sites lies in their weight, influenced by the thickness and density of the vegetation cover. This structural design allows us to evaluate the influence of vegetation density and layer depth on runoff reduction and green roof efficiency.

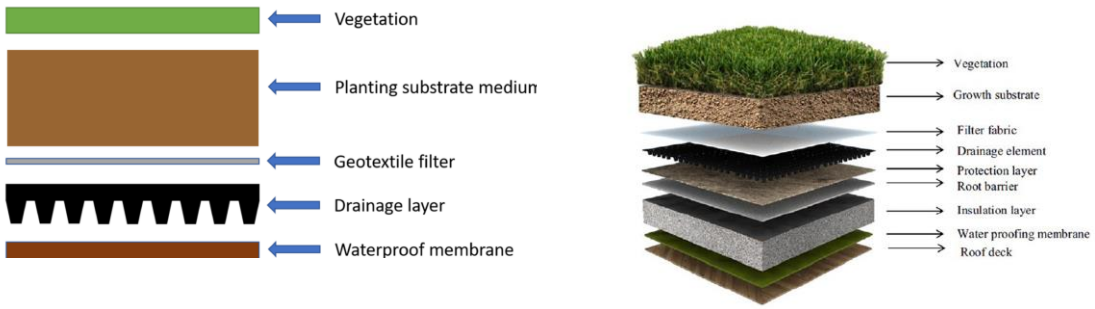

Figure 4. Typical structure of a green roof (Basu et al., 2022; Basu et al., 2021).

To evaluate the green roof system for different vegetation cover type we replaced sedum with turf for two of Rosemount cradles on April 15, 2024. Dataset collection (Figure, 5).

Figure 5. Implemented green roof cradles at UCD: two cradles with green vegetation cover are Turf (right cradles), and the remaining two are Sedum (left cradles).

3. Equipment

The green roof system and mini weather station (Ecomet 2) collected data including dry temperature ,surface temperature, subsurface temperature, soil moisture, cradle weight, runoff discharge, air temperature, relative humidity, precipitation (radar based), water vapor pressure, air pressure, wind speed and wind direction. To collect the green roof and metrological dataset, an IoT based AquaRoot Control System (ARCS) implemented. ARCS is a supervisory control and data acquisition (SCADA) software system dedicated to data acquisition, data storage and representation in autonomous distributed IoT sensors networks (Figure 6).

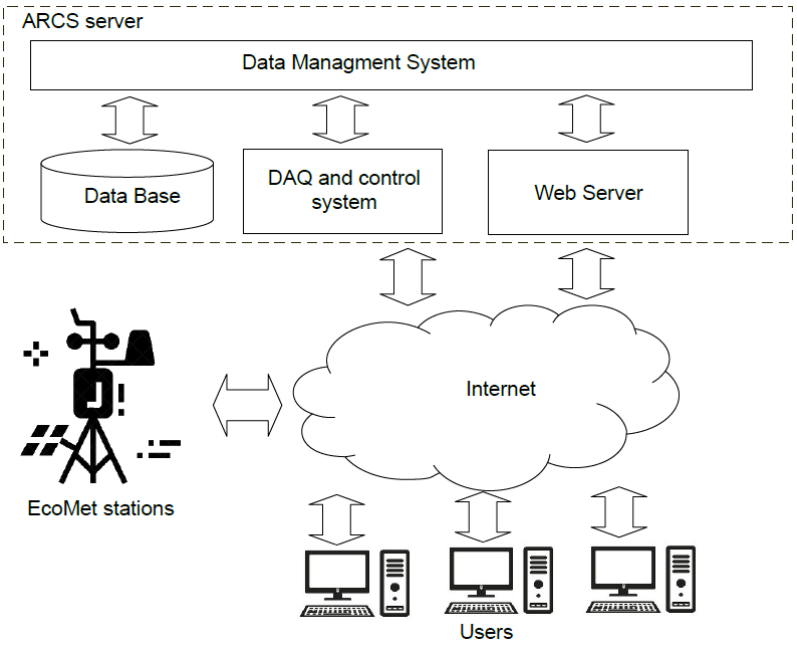

Figure 6. AquaRoot Control System architecture and IoT devices connectivity

It is based on a stable multi-user software platform, provided real-time access to the data acquired. ARCS software is based on a distributed client-server technology. It consists of Data acquisition (DAQ) server, real-time database, user interface, web-server and security system which form WorkStation (data server). IoT devices connect the DAQ server as clients and exchange with the information with it. Database managing system is accepting DAQ data and archiving them into

data base. User interface and web-server system allows to represent the real-time data to the user. Web browser is used as a client software to connect ARCS server, visualize current and archived data. Some users may connect ARCS simultaneously by their web-browsers and work with the server independently (Figure 7 and 8). Figure (7) depicts multiple parts of the main screen software of the AquaRoot Control System, including instant sensor measurements, observation units, and other system settings. Figure (8) represents the AquaRoot Control System data logger, which is used for exporting recorded datasets in CSV format.

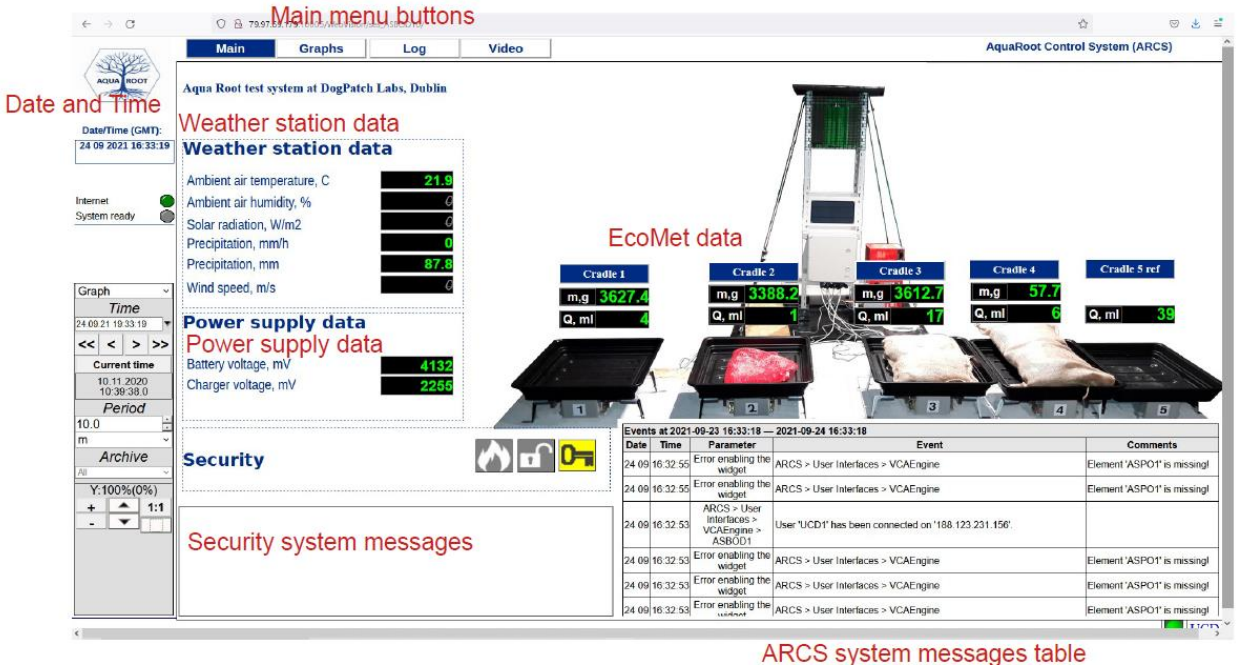

Figure 7. AquaRoot Control System main screen

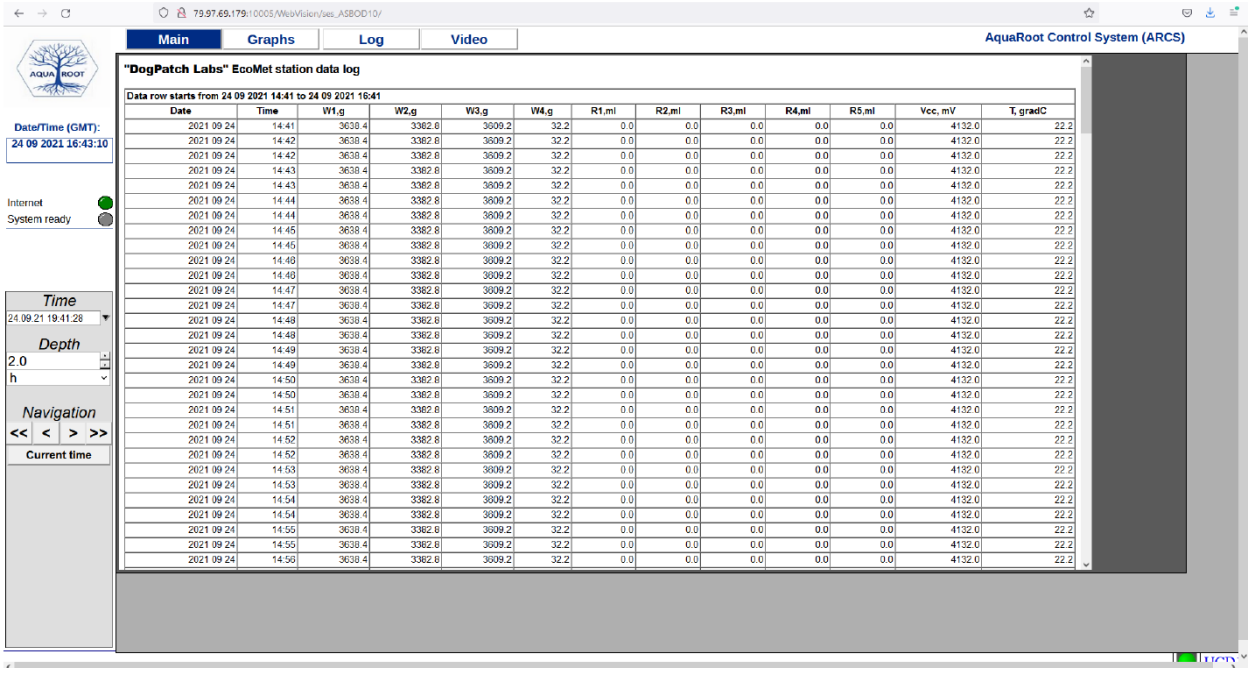

Figure 8. AquaRoot Control System data logger

4. Results

Historical data from Dublin Airport (1943–2024) indicates that rain occurred on 57.4% of days, with an average daily rainfall of 3.6 mm and a duration of 5.1 hours. Average temperature and humidity were 9.63°C and 82.15%, respectively, with 4.01 hours of sunlight. Dublin's humid climate and frequent rainfall underscore the need for runoff control strategies to mitigate flood risks (Lhomme et al., 2019; Paranunzio et al., 2022; Pilla et al., 2019)

4.1 Rainfall and runoff parameters statistics

Table 3 presents rainfall characteristics for the study events in Rosemount site. TRAV, RIP, RAD, and RAMI had mean values of 3.35 mm, 1.37 mm/h, 7.0 hours, and 0.47 mm/h, respectively, with positive skewness, indicating variability in precipitation intensity and duration. This variability is critical in evaluating the green roof's performance under diverse rainfall conditions.

Table 3. Statistical characteristics of rainfall in the studied events.

Rainfall characteristics	Min	Max	Mean	Median	SD

TRAV (mm)	0.17	19.1	4.51	3.25	4.29
RIP (mm/h)	0.08	6.5	1.62	1.3	1.44
RAD (h)	2	14	7.24	7	3.38
RAMI (mm/h)	0.03	2.39	0.60	0.48	0.5

Table 4 presents the statistical characteristics of climatic conditions and green roof weights during precipitation events. Relative humidity, air temperature, and wind speed averaged 79.54%, 11.75°C, and 1 m/s, respectively. The weight of the green roof system showed an increase from an average of 40.8 kg at the beginning of rainfall events (BWS) to 42.91 kg at peak precipitation (MBW), before settling at 42.15 kg by the end of the events (BWE). This increase in weight reflects the green roof's water absorption capability, as it retains precipitation during events. The slight skewness observed in the weight distribution at different stages of events suggests consistent retention and release patterns, likely influenced by microclimate variations across the sites. In addition, Minor variances compared to nearby Met Éireann stations indicate local microclimate influences. a slight negative skewness.

Table 4. Statistical characteristics of climatic parameters and green roof weight for the studied events.

Weather parameters and box weight	Min	Max	Mean	Median	SD
RH (%)	59	97	79.54	80	9.05
AT (°C)	2.5	23	11.68	11.75	4.54
WS (m/s)	0	3	1.16	1	0.78
BWS (kg)	32.93	45.2	40.8	41.27	2.92
MBW (kg)	33.95	46.3	42.91	43.02	2.25
BWE (kg)	33.25	45.85	42.15	42.34	2.2
NRPO (h)	2	105	20.54	10.5	25.08

The green roof system's hydrological performance, detailed in Table 5, shows an average delay of 2.34 hours for the start of runoff (RORD) and 1.74 hours for peak runoff (RPDRP) relative to

rainfall start and peak, respectively. This delay in runoff helps to mitigate the immediate impact of rainfall on drainage systems. Moreover, the green roof reduced peak runoff intensity (RUPFM) by 0.9 mm/h compared to average rainfall intensity, highlighting its capacity to buffer intense rain events. Water Retention Percentage (WRP) averaged 55.69%, with values ranging from 8.57% to 100% across events, indicating that the green roof can retain substantial rainfall, though performance varies with rainfall intensity and duration.

Table 5. Statistical characteristics of runoff hydrological parameters for the studied events.

Runoff characteristics	Min	Max	Mean	Median	SD
TRUV (mm)	0	13.25	2.45	1.83	2.67
TRD (h)	0	13	6.78	7	3.5
RUPFM (mm/h)	0	3.2	0.9	0.72	0.88
RORD (h)	0	9	2.34	2	2.13
RPDRP (h)	0	8	1.74	1	1.65
PFR (mm/h)	0.04	3.3	0.73	0.45	0.71
WRA (mm)	0.13	8.6	2.05	1.29	1.88
WRP (%)	8.57	100	55.69	48.52	24.75

The average runoff characteristics for various rainfall intensity classes are summarized in Table 6, showing that rainfall parameters significantly impact the green roof system's retention performance. For events with TRAV (Total Rainfall Amount) below 1.5 mm, the green roof retained approximately 74.9% of precipitation, while retention decreased to 61.65% for TRAV between 1.5 and 3 mm and to 42.6% for TRAV above 6 mm. As precipitation characteristics like TRAV, RIP (Rainfall Intensity Peak), RAD (Rainfall Duration), and RAMI (Rainfall Intensity Mean) increased, corresponding runoff parameters such as WRA (Water Retention Amount), TRUV (Total Runoff Volume), RUPFM (Runoff Peak Flow Maximum), and PRF (Peak Runoff Flow) also showed increases. For instance, in events with TRAV less than 1.5 mm, WRA, TRUV, RUPFM, and PRF averaged 0.6, 0.21, 0.08, and 0.34 mm, respectively, compared to 3.26, 4.45, 1.9, and 1.24 mm for events where TRAV exceeded 6 mm. Similarly, increases in RIP, RAD, and

RAMI were associated with higher averages in runoff metrics, emphasizing the green roof's varying retention capacity across rainfall intensities.

Table 6. Average runoff characteristics in various classes of rainfall characteristics for different events

		WRA (mm)	WPA (%)	TRUV (mm)	TRD (h)	RUPFM (mm)	RORD (h)	PFR (mm)	PRP (%)
TRAV (mm)	0.0 1.5	0.57	74.92	0.2	3.47	0.09	2.67	0.36	82.78
	1.5_3.0	1.24	61.03	0.91	6	0.41	1.29	0.53	59.53
	3.0_4.5	1.43	40.59	2.11	6.75	1.05	3	0.38	25.1
	4.5_6	2	38.52	3.1	9.71	1.15	2.14	0.65	39.64
	>6.0	4.44	44.53	5.65	9.46	1.94	2.46	1.41	38.23
IRP (mm/h)	0.0_0.5	0.59	74.4	0.21	3.82	0.08	3.09	0.26	80.76
	0.05_1.0	1.02	73.6	0.46	4.14	0.16	2.71	0.42	70.4
	1.0_1.5	1.79	54.41	1.66	8	0.51	2.29	0.64	56.09
	1.5_2.0	2.11	40.64	2.98	8.25	1.14	1.75	0.55	33.06
	>2.0	3.97	40.18	5.54	9.15	2.07	1.92	1.45	38.07
RAD (h)	2_4	0.75	62.88	0.66	4.29	0.4	0.71	0.56	73.28
	4_6	1.33	71.36	0.98	3.56	0.51	2.11	0.52	69.25
	6_8	1.69	49.17	2.29	6.56	1.05	1.89	0.8	49.86
	8_10	2.01	47.75	3.46	7.86	1.03	2.57	0.79	46.69
	>10	3.44	50.2	3.91	9.71	1.25	3.5	0.87	44.39
RAMI (mm/h)	0.0_0.25	0.63	76.94	0.2	3.55	0.07	3.45	0.26	78.24
	0.25_0.50	1.26	60.89	1.01	6.08	0.33	2.42	0.49	65.03
	0.50_0.75	1.73	40.28	2.92	9.11	1.21	1.11	0.78	42.45
	0.75_1.0	3.56	43.85	4.75	9.29	1.7	2.71	0.7	30.07
	>1.0	4.57	45.07	5.6	7.57	2.02	1.71	1.82	42.83

Table 7 displays the correlation coefficients between rainfall parameters and runoff characteristics, revealing that Total Rainfall Amount (TRAV) has the strongest correlations with runoff metrics, particularly TRUV (Total Runoff Volume) at 0.96, followed by WRA (Water Retention Amount) at 0.91 and RUPFM (Runoff Peak Flow Maximum) at 0.86. These values indicate that TRAV heavily influences overall runoff volume. Rainfall Intensity Peak (RIP) also correlates strongly with RUPFM and TRUV, suggesting that intense rainfall drives higher peak flows and runoff volumes. Interestingly, RIP shows an inverse relationship with delay metrics RPDRP and RORD, implying that higher rainfall intensity reduces the delay before runoff peaks. Rainfall Duration

(RAD) has a moderate correlation with TRD (Total Runoff Duration) at 0.69, while RAMI (Rainfall Intensity Mean) shows weaker but still notable correlations with WRA and RUPFM. The Nighttime Roof Precipitation Offset (NRPO) influences delay metrics, with correlations of 0.46 and 0.58 for RORD and RPDRP, respectively, suggesting it affects the initial dryness of the substrate. In contrast, weather parameters exhibit lower correlations overall, with the highest being air temperature's correlation with WRA and PRF at only 0.35, indicating that rainfall characteristics are the primary drivers of runoff behavior on the green roof system.

Table 7. Estimated correlation coefficient value between runoff characteristics and rainfall characteristics and weather parameters.

R^2	WRA (mm)	TRUV (mm)	TRD (h)	RUPFM (mm)	RORD (h)	RPDRP (h)	PFR (mm)
TRAV (mm)	0.91	0.96	0.63	0.86	0.03	-0.16	0.73
RIP (mm/h)	0.78	0.87	0.49	0.92	-0.14	-0.32	0.88
RAD (h)	0.54	0.52	0.69	0.40	0.42	0.17	0.17
RAMI (mm/h)	0.75	0.80	0.36	0.81	-0.19	-0.29	0.75
NRPO (h)	-0.09	-0.27	-0.36	-0.34	0.46	0.58	-0.12
RH (%)	0.16	0.03	0.01	0.01	-0.01	0.01	-0.11
AT (°C)	0.35	0.33	-0.10	0.25	0.16	0.10	0.35
WS (m/s)	-0.25	-0.07	-0.08	0.01	0.01	0.21	-0.09

4.2 Machine learning based runoff characteristics modeling result.

Based on the 46 rainfall event XGBoost (XGB), Random Forest regression (RF), and Support Vector Regression (SVR) machine learning algorithms implemented to model the main runoff characteristics based on the independent variables including the TRAV, RIP, RAD, RAMI, NRPO, RH, AT, WS. The runoff characteristics as dependent variables including WRA, TRUV, TRD, RUPFM, RORD, RPDRP, and PFR. To optimize model performance, various combinations of independent variables were tested across each model to identify the most influential predictors for each runoff characteristic. Detailed methodology and implementation results are provided in Appendix A and B.

Table 8. Number of variables repetition in different ML implementation with higher R^2 and lower RMSE

	TRAV	RIP	RAD	RAMI	NRPO	RH	AT	WS
WRA	24	13	15	13	24	9	14	8
TRUV	24	11	15	14	18	11	13	15

TRD	24	24	24	13	18	7	19	5
RUPFM	12	24	18	13	16	16	16	5
PFR	6	24	14	14	22	8	13	12
Sum	90	96	86	67	98	51	75	45
Percentage %	75	80	71.67	55.83	81.67	42.5	62.5	37.5

Table 8 summarizes the frequency with which each independent variable was selected across various model configurations and combinations in the XGBoost, Random Forest, and Support Vector Regression algorithms. With a maximum possible repetition of 24, Nighttime Roof Precipitation Offset (NRPO) appeared in 81.67% of configurations, underscoring its significance in predicting runoff characteristics. Rainfall Intensity Peak (RIP) and Total Rainfall Amount (TRAV) were also highly influential, with repetition rates of 80% and 75%, respectively, followed by Air Temperature (AT), Rainfall Intensity Mean (RAMI), Relative Humidity (RH), and Wind Speed (WS), with decreasing levels of importance. Figure 9illustrates model performance, showing R^2 and RMSE values for each algorithm as the number of independent variables varies. Overall, NRPO, RIP, and TRAV emerged as the most critical predictors, indicating their primary influence on runoff behavior. The next section will discuss model results for each runoff characteristic in detail.

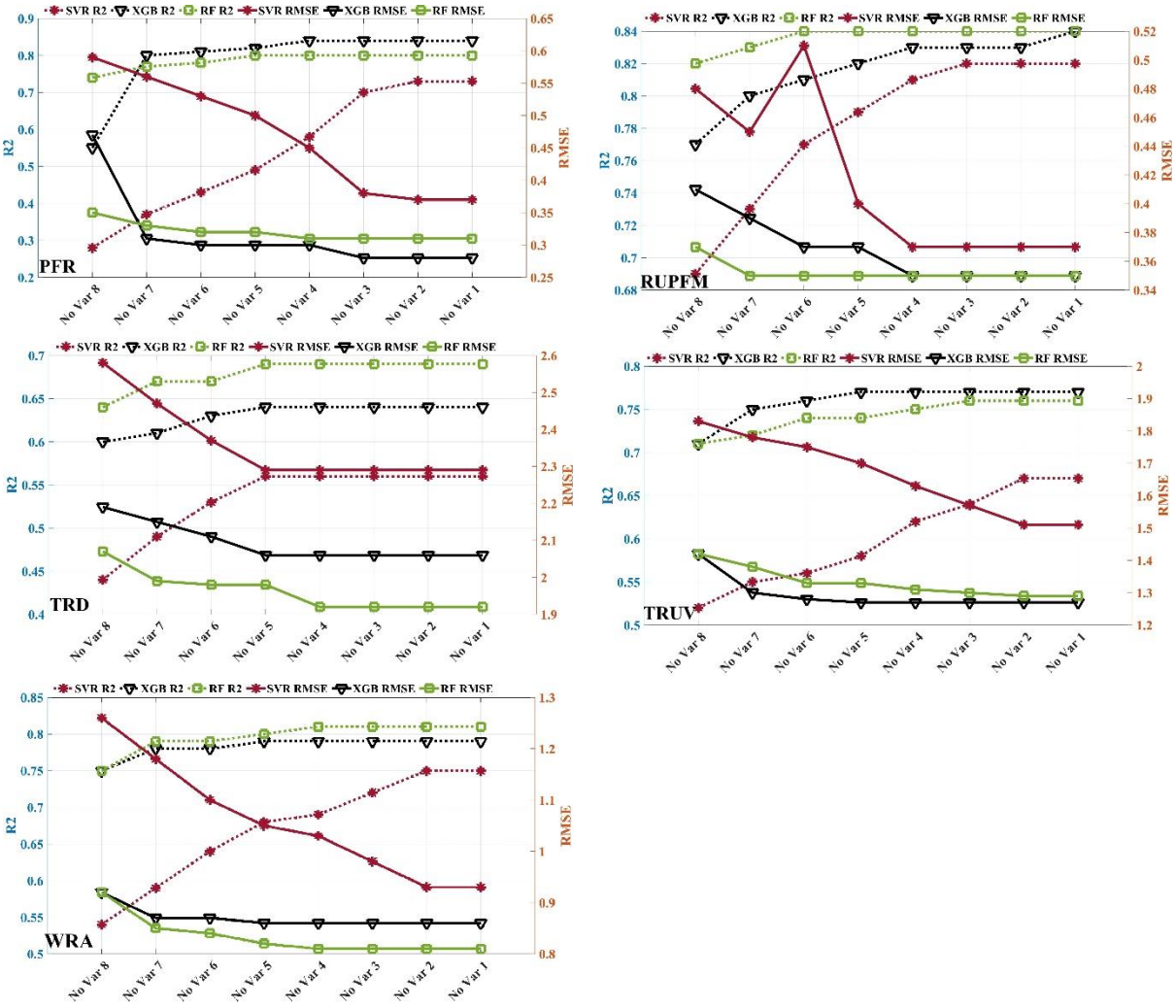

Figure 9. Different ML implementation for runoff characteristic with different variables combination (left y-axis is R^2 value, right y-axis is RMSE value, x-axis is number of variables used in modeling).

Peak Flow Reduction (PFR): For PFR modeling, the SVR model showed an improvement in R^2 from 0.27 to 0.7 as the number of variables decreased from 8 to 3, with RMSE correspondingly decreasing. Beyond 3 variables, R^2 and RMSE changes were minimal, indicating that the remaining three variables are sufficient for effective modeling. In the XGB model, removing one variable from the initial 8 led to a marked improvement, suggesting the presence of an irrelevant variable. XGB achieved the highest R^2 (0.84) and lowest RMSE (0.27), outperforming SVR and RF in predictive accuracy. The RF model demonstrated stable performance with minimal fluctuations in R^2 and RMSE as variables were reduced, underscoring its robustness in handling heterogeneous variables. RF's R^2 increased steadily from 8 to 5 variables, stabilizing at 0.8, with

RMSE similarly stabilizing at 0.3 after an initial decrease. According to Table 8, RIP and NRPO were the most influential variables in PFR modeling, while TRAV had minimal impact. RAD and RAMI contributed equally, indicating their balanced importance in the model.

RUnoff Peak Flow Maximum (RUPFM): In the SVR model for RUPFM, R^2 increased from 0.69 to 0.82 as variables were reduced from 8 to 3, with R^2 stabilizing beyond this point. RMSE also decreased consistently from 8 to 4 variables, with a noticeable shift at 6 variables, likely reflecting the model's sensitivity to optimal variable combinations. For the XGB model, R^2 improved significantly from 0.77 to 0.83 as variables were reduced from 8 to 4, with RMSE stabilizing at 5 variables at 0.35, aligning with the RF model's RMSE. The RF model showed the highest R^2, reaching 0.84 with 6 variables, and demonstrated stability in RMSE beyond 7 variables. Overall, RF provided the best predictive accuracy with the highest R^2 and lowest RMSE among the models (Figure 9). In RUPFM modeling, RIP emerged as the most influential predictor, while Wind Speed (WS) showed the least impact on model performance.

Total Runoff Duration (TRD): For TRD modeling, all three models—XGB, RF, and SVR—showed notable improvements in R^2 and reductions in RMSE as the number of variables decreased from 8 to 5. Specifically, R^2 values increased for XGB from 0.6 to 0.64, for RF from 0.64 to 0.69, and for SVR from 0.44 to 0.56. Beyond 5 variables, R^2 and RMSE values stabilized, with only a minor R^2 change for RF when reduced to 4 variables (Figure 9). Among the models, RF achieved the highest R^2 and lowest RMSE, indicating superior predictive accuracy for TRD. Table 8 highlights that TRAV, RIP, and RAD were the most influential predictors across all scenarios, underscoring their importance in TRD modeling, while Wind Speed (WS) had the least impact on model performance.

Total RUnoff Volume (TRUV): For TRUV modeling, XGB and RF models showed similar R^2 trends, with XGB performing slightly better. XGB's R^2 increased from 0.71 to 0.77 as the number of variables was reduced from 8 to 5, while RF's R^2 rose from 0.71 to 0.76, with the most noticeable improvement occurring from 8 to 3 variables. SVR displayed more variability, with R^2 starting at 0.52 for 8 variables and gradually increasing to 0.67 with 2 variables before stabilizing. RMSE trends mirrored the R^2 changes across all models (Figure 11). Overall, XGB emerged as the best model for TRUV, achieving the highest R^2 and lowest RMSE. According to Table 8,

TRAV had the most substantial influence on TRUV predictions, whereas RIP and Relative Humidity (RH) showed minimal impact.

Water Retention Amount (WRA): For WRA modeling, SVR showed a significant R^2 increase from 0.54 to 0.75 as the number of variables was reduced from 8 to 2, with R^2 and RMSE stabilizing beyond 2 variables. RF and XGB models exhibited similar trends, with R^2 values rising from 0.75 to 0.81 for RF and 0.79 for XGB as variables were reduced from 8 to 4. RMSE values for both models decreased correspondingly before stabilizing (Figure 11). Overall, RF achieved the best performance for WRA, with the highest R^2 and lowest RMSE among the three models. According to Table 8, NRPO and TRAV were the most influential predictors for WRA, while RAD had the least impact on the model's performance.

5. Conclusion

This study demonstrates the effectiveness of green roof systems in Dublin as a Nature-Based Solution (NBS) for urban runoff management, particularly through machine learning applications. By centering on advanced, event-based measurements and machine learning models, this research provides actionable insights for urban environmental planning. Our findings reveal green roofs' substantial potential to reduce runoff volume, delay peak flow, and improve urban resilience against flooding.

A notable insight is the influence of Dublin's diverse microclimatic conditions on green roof performance. Localized differences in humidity, wind speed, temperature, and sunlight exposure result in variations in water retention and runoff delay, underscoring the need for site-specific designs. Our study recorded average relative humidity, air temperature, and wind speed at green roof sites as 79.54%, 11.75°C, and 1 m/s, respectively, slightly diverging from data at Met Éireann's Dublin Airport and Phoenix Park stations. These discrepancies emphasize the importance of localized data collection, which not only improves environmental modeling accuracy but also aligns with Building Regulations, ensuring that designs address Dublin's unique climate conditions. Moreover, meeting Building Regulations—such as those governing load-bearing capacity, drainage, and waterproofing—ensures structural safety and enhances green roofs' long-term viability as flood mitigation and sustainability tools.

Our research also highlights the benefits of a double-layer green roof configuration, which provides greater water retention and peak runoff reduction, offering further support for stormwater management. Beyond hydrological impacts, green roofs improve air quality, promote biodiversity, and enhance urban aesthetics, contributing to residents' quality of life. Nevertheless, challenges remain, such as managing non-biodegradable materials, meeting structural standards, and balancing the increased costs of construction and maintenance.

This study's machine learning focus, employing XGBoost (XGB), Random Forest (RF), and Support Vector Regression (SVR), revealed these models' superiority over traditional mathematical approaches in capturing complex meteorological-runoff relationships. XGB and RF consistently outperformed SVR, accurately predicting runoff characteristics with robust modeling of influential variables like Total Rainfall Volume (TRAV), Rainfall Intensity at Peak (RIP), and Nighttime Roof Precipitation Offset (NRPO). This underscores machine learning's role in advancing data-driven solutions for urban stormwater management.

Future research should explore long-term green roof performance under varied climate conditions, particularly during extreme weather, to enhance resilience planning. Examining vegetation types and soil compositions may offer design customizations for different climates, while advanced modeling techniques, like deep learning, could improve predictive accuracy. Additionally, future studies could investigate the potential for biodegradable materials and sustainable practices to lower environmental impact and better align with regulatory standards.

In conclusion, this study's data-driven approach underscores the importance of green roofs in sustainable urban design. By integrating machine learning to predict runoff dynamics accurately, it provides a framework for leveraging green infrastructure to mitigate urban runoff effectively. Emphasizing site-specific microclimate data and regulatory compliance ensures that green roofs are optimized for both hydrological benefits and structural safety, supporting their role as essential components in resilient, climate-adaptive urban landscapes.

.

Acknowledgments

We extend our appreciation to Vincent Farrelly of AquaRoot Technologies Ltd and Yury Murashev of Energy Harvesting Solutions Ltd for their valuable technical support and advice throughout all stages of this project, from initial design to hardware and software development, installation, maintenance, and data capture and analysis.

Additionally, special thanks go to Neil Menzies and his colleagues at Hibernia Real Estate for generously providing rooftop locations in Dublin city for the EcoMet green roof monitors and their ongoing support and interest in this project.

Appendix A : Methodology and dataset analysis

The overall procedure for modeling the runoff characteristics and extracting parameters for the green roof system in this study is illustrated in Figure A1.

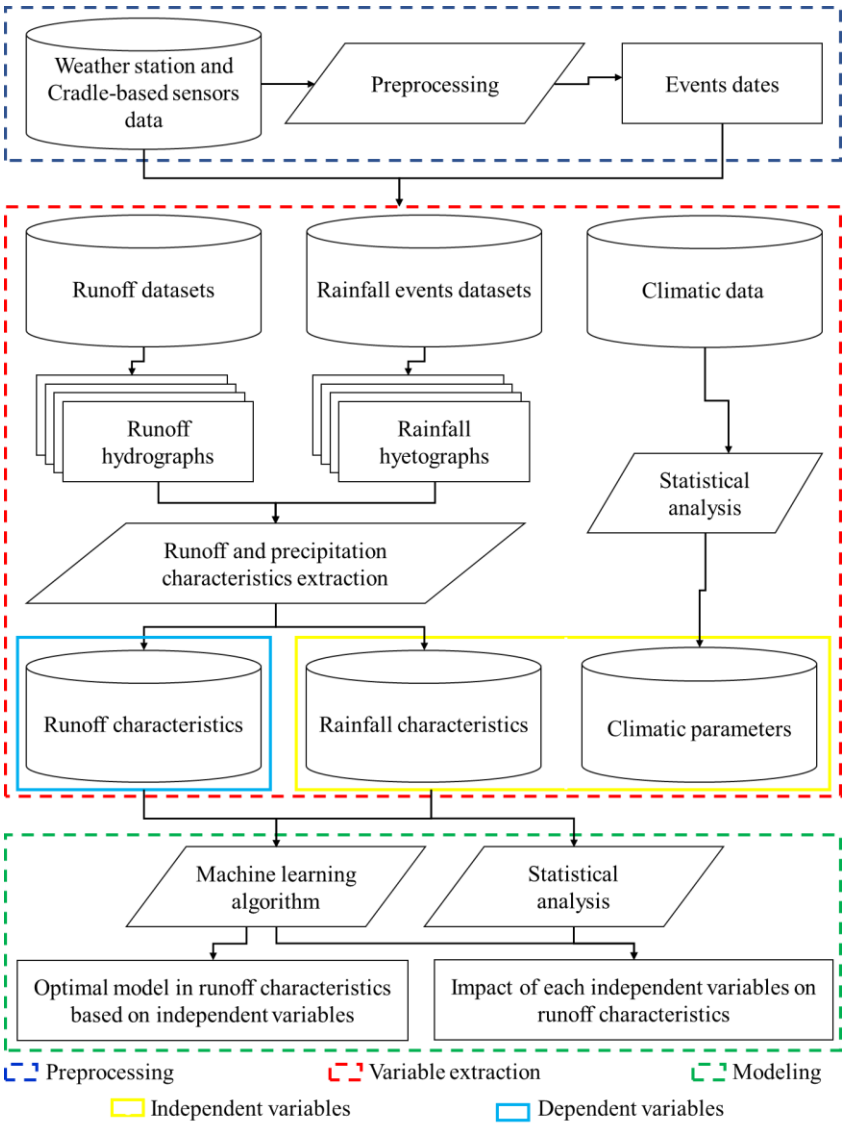

Figure A1. Diagram of the methodology

A.1 Rainfall and Runoff characteristics extraction

The data analysis was conducted using a step-by-step approach. In the first step, the recorded rainfall and runoff data were analyzed to identify each significant rainfall event that occurred during the study period. The end of each rainfall event was defined as the time when at least 2 hours passed without rainfall after each event (Soulis & Valiantzas, 2012). A total of 46 rainfall events were recorded during the study period. The average value of valid measurements from the four green roof datasets was considered as the main parameter for the green roof measurements.

Datasets related to rainfall, runoff, and climatic data were extracted from the raw data, corresponding to the time of occurrence of selected rainfall events. In the second step, information on various characteristics of rainfall was extracted based on the hyetograph of each rainfall event. Then, in the next step, various characteristics were calculated for each rainfall event based on the runoff hydrographs obtained from the cradle with the green roof (Mentens et al., 2006; Palla et al., 2011; Speak et al., 2013; Stovin et al., 2013). The details of the parameters calculated from the rainfall hyetograph and runoff hydrograph are shown in and Table (A1) and Figure (A2). Additionally, in this step, the following parameters were extracted for each event: average climatic parameters (RH, WS, AT) and cradle weight-based parameters (Box Weight at Rainfall Start, BWS; Maximum Box Weight during Rainfall, MBW; and Box Weight at Rainfall End, BWE). Furthermore, the following parameters were extracted based on the rainfall hyetograph and runoff hydrograph (see Table A1): RAinfall Duration (RAD), Total RAinfall Volume (TRAV), Rainfall Intensity at Peak (RIP), RAinfall Mean Intensity (RAMI), No Rainfall Period to Onset (NRPO), Total RUnoff Volume (TRUV), RUnoff Peak Flow Maximum (RUPFM), Runoff Peak Delay to Rainfall Peak (RPDRP), Peak Flow Reduction (PFR), Peak Runoff Reduction Percentage (PRP), Rainfall Onset to Runoff Onset Delay (RORD), Total Runoff Duration (TRD), Water Retention Amount (WRA), Water Retention Percentage (WRP).

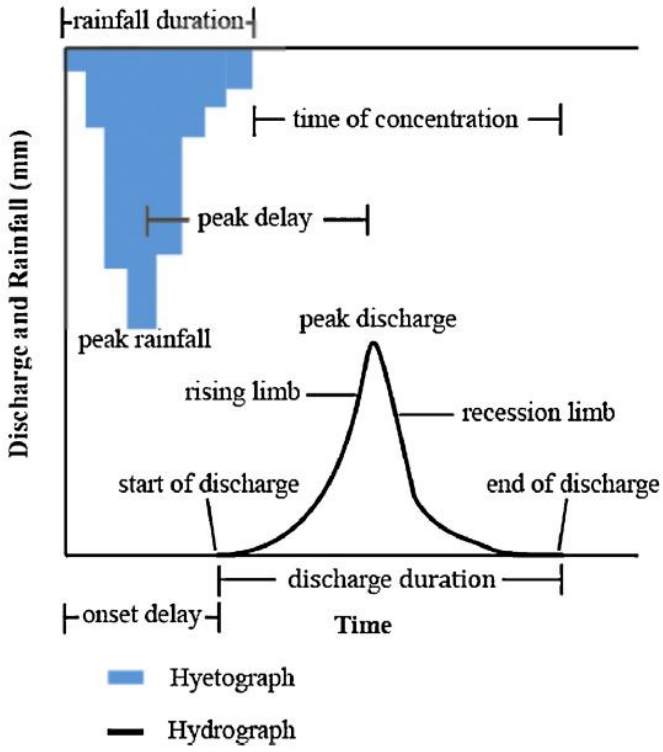

Figure A2. Annotated diagram explaining hydrologic terms pertaining to rainfall and discharge response in the analysis (Wong & Jim, 2014).

Table A1. Details of the calculated parameters from the rainfall hyetograph and runoff hydrograph for the rainfall event.

Characteristics	Description	Unit	References
RAinfall Duration (RAD)	The total duration of rainfall.	h	(Mentens et al., 2006; Nawaz et al., 2015; Palla et al., 2011; Soulis et al., 2017; Speak et al., 2013; Stovin et al., 2013; Wong & Jim, 2014)
Total RAinfall Volume (TRAV)	The amount of total rain falling within rainfall duration.	mm	
Rainfall Intensity at Peak (RIP)	The rainfall rate for peak rainfall.	mm/h	
RAinfall Mean Intensity (RAMI)	The average rainfall rate for rainfall duration.	mm/h	
No Rainfall Period to Onset (NRPO)	The dry weather period between two independent rainfall events (from previous event).	h	
Total RUnoff Volume (TRUV)	The amount of total runoff within runoff discharge duration.	mm	
RUnoff Peak Flow Maximum (RUPFM)	The maximum rate of discharge during the period of runoff.	mm/h	

Runoff Peak Delay to Rainfall Peak (RPDRP)	The time difference between the peak of rainfall and the peak of discharge.	h
Peak Flow Reduction (PFR)	The absolute value of reduced peak discharge intensity relative to the respective peak rainfall intensity.	mm/h
Peak Runoff Reduction Percentage (PRP)	The percentage of reduced peak discharge intensity relative to the respective peak rainfall intensity.	%
Rainfall Onset to Runoff Onset Delay (RORD)	The time difference between the start of rainfall and the start of discharge.	h
Total Runoff Duration (TRD)	The total duration of discharge.	h
Water Retention Amount (WRA)	The volume of rainwater retention by the green roof system	mm
Water Retention Percentage (WRP)	The percentage of rainfall retention by the green roof system to the total volume of rainfall	%

A.2 Statistical and machine learning implementation for runoff characteristics modeling

In our study, we employed statistical and machine learning algorithms to model runoff characteristics, focusing on understanding the relationship between various weather parameters and runoff behavior. Initially, we conducted a univariate analysis to evaluate the average runoff characteristics under different weather conditions, providing insights into the basic impacts of each weather parameter. Additionally, we calculated correlation coefficients between independent variables (weather parameters) and dependent variables (runoff characteristics) to assess the explanatory power of the weather parameters in predicting runoff behavior. To further enhance our analysis, we utilized three advanced machine learning algorithms: Random Forest regression, XGBoost regression, and Support Vector Regression (SVR). These algorithms allowed us to consider multivariate factors and capture nonlinear relationships between weather parameters and runoff characteristics.

Random Forest (RF) regression is an ensemble learning method that combines multiple decision trees to model nonlinear relationships. RF is particularly useful in hydrological modeling due to

its ability to rank the importance of variables and its robustness against overfitting. XGBoost regression represents an advanced evolution of gradient boosting algorithms, optimized for computational efficiency and model performance. It effectively handles complex interactions in environmental data and prevents overfitting through regularization. Support Vector Regression (SVR) builds upon Support Vector Machines (SVMs) principles, offering robust performance in regression tasks by mapping input data features into a higher-dimensional space and seeking a hyperplane that best fits the data. SVR is valuable for managing noise in complex datasets and achieving robust generalization in environmental modeling. Overall, these algorithms allow for comprehensive analysis and accurate prediction of runoff characteristics, essential for effective green roof system management and environmental planning.

In the modeling process, different rainfall characteristics (intensity and duration) and weather parameters (temperature and humidity) were considered as independent variables. Runoff characteristics were treated as dependent variables. In the univariate evaluation, the average of different runoff characteristics including peak runoff, total volume, and delay time, were designated as dependent variables. Initially, a univariate analysis was conducted where the average of various runoff characteristics was calculated for different classes of independent variables. This step is essential in understanding the basic impacts of each weather parameter on runoff behavior. To further justify the methodology, the correlation coefficient was calculated between each independent variable and runoff hydrograph characteristics. This measure helps assess the explanatory power of the independent variables concerning the dependent variables, providing a preliminary indication of relevant predictors. Furthermore, we employed three advanced machine learning algorithms for more comprehensive analysis, considering multivariate factors including random forest regression (RF), XGBoost (XGB), and Support Vector Regression (SVR)(Adnan et al., 2021; Behzad et al., 2009; Chen & Pang, 2019; Chen et al., 2015; Le et al., 2019; X. Li et al., 2019; Man et al., 2018; Marjanović et al., 2011; Tehrany et al., 2014; Yao et al., 2008). The runoff models are validated using the Leave-One-Out Cross-Validation (LOOCV) method, which is particularly suitable for small datasets. This method helps in assessing the model's generalization capabilities and provides an unbiased estimate of the model performance by systematically leaving out one sample at a time from the training process (Dinh & Aires, 2022; Rennie, 2003; Sreedharan et al., 2023). In LOOCV, the model is trained on all but one of the data points, and the left-out point is used as the test set. This process is repeated such that each data point serves as the test set

exactly once. This approach is particularly valuable in hydrological modeling where data can often be scarce or highly variable across different conditions (Mukonza & Chiang, 2022). It helps in identifying outliers or data points that are particularly influential to the model, which is crucial for hydrological models where certain extreme events (like heavy rainfall) might be underrepresented. In the next step, the importance of the variables was evaluated by analyzing combinations that produced the highest R^2 and the lowest Root Mean Square Error (RMSE). These metrics are essential for fine-tuning the models and selecting the most impactful predictors. The performance of the final models was then quantified by comparing the observed with the modeled runoff characteristics using both R^2 and RMSE as indicators of accuracy.

A.2.1 Random Forest (RF) Regression

RF is a powerful ensemble learning method utilized to model the nonlinear relationships between independent variables (e.g., climatic parameters and rainfall characteristics) and dependent variables (e.g., runoff characteristics in green roof systems). This method combines multiple decision trees to form a "forest," trained on random subsets of the data with replacement, a technique known as bootstrapping (Breiman, 2001; Pourghasemi & Kerle, 2016; Sagi & Rokach, 2018). Each tree in a Random Forest is built from a random sample of the data, ensuring that each tree develops unique insights about the dataset, which reduces the correlation between the trees and increases the model's general robustness against overfitting (Breiman, 2001; Micheletti et al., 2014; Mienye & Sun, 2022). In the Random Forest, each decision tree operates on a random subset of features to determine splits, further enhancing the diversity among the trees and thereby the generalization ability of the model (Li et al., 2022). When making predictions, Random Forest aggregates the predictions from individual trees through majority voting or averaging, which mitigates the noise and variance associated with individual trees (Solomon et al., 2023). This aggregation helps in achieving more stable and accurate predictions, especially beneficial in hydrological modeling where the response to climatic variables can be highly non-linear and complex (Guo et al., 2021; Xiang et al., 2021) An intrinsic advantage of using RF is its ability to rank the importance of variables based on how much they improve the purity of the node, which helps in understanding which variables are the most influential in predicting runoff characteristics. This feature is crucial for interpreting hydrological data, as it allows researchers to identify the most significant climatic factors affecting runoff dynamics (Yang & Chui, 2021). The detailed

explanation and mathematical formulation of RF algorithm can be found Belgiu and Drăguţ (2016); Breiman (2001).

A.2.2 XGBoost Regression

XGBoost represents an advanced evolution of gradient boosting algorithms, designed to optimize both computational efficiency and model performance. XGBoost enhances the sequential combination of weak learners, typically decision trees, to construct a robust predictive model (Nielsen, 2016). In XGBoost, trees are built sequentially, with each new tree correcting errors made by the previous trees in the series. This approach effectively reduces bias and improves the model's accuracy with each iteration. A key feature that sets XGBoost apart from traditional gradient boosting is the incorporation of a regularization term in its objective function. This regularization helps control the complexity of the model, preventing overfitting—a common challenge in predictive modeling. This makes XGBoost particularly useful in hydrological modeling, where the prevention of overfitting is crucial due to the often-limited size of datasets and the complexity of interactions in environmental data (Chen & Guestrin, 2016; Chen et al., 2015; Yang & Chui, 2021). Unlike other boosting methods that stop growing trees when they reach a maximum depth, XGBoost uses a more nuanced "tree pruning" technique. Trees are grown to their maximum depth and then pruned back to remove splits that provide little gain, enhancing the model's efficiency and interpretability (Chen & Guestrin, 2016). XGBoost is renowned for its execution speed and model performance, attributes that are attributed to its unique handling of tree pruning and its ability to perform parallel computation on single machines. Its efficiency makes it an excellent choice for complex hydrological models where multiple variables and large datasets are common. The structured nature of hydrological data, with variables like rainfall, temperature, and soil moisture, makes XGBoost an ideal tool for this domain. Its ability to handle tabular data effectively allows it to model complex relationships between multiple input features and the target variable (Keck, 2016; Y. Li et al., 2019), which in this context is the runoff characteristics from green roof systems. The detailed explanation and mathematical formulation of XGBoost algorithm can be found in Chen and Guestrin (2016); Chen et al. (2015); Friedman (2001).

A.2.3 Support Vector Regression (SVR)

Support Vector Regression (SVR) builds upon the principles of Support Vector Machines (SVMs), which are primarily known for their robust performance in classification tasks. SVM are non-

parametric, kernel-based methods that originate from statistical learning theory (Vapnik & Vapnik, 1998). They are especially useful for addressing nonlinear, high-dimensional problems in classification, regression, and density estimation robustly by managing the complexity of the model (Behzad et al., 2009; Cherkassky & Mulier, 2007; Micheletti et al., 2014; Moguerza & Muñoz, 2006; Mountrakis et al., 2011; Tehrany et al., 2014; Wan & Lei, 2009). SVR operates by mapping input data features into a higher-dimensional space using a kernel function (Marjanović et al., 2011; Tehrany et al., 2014). In this transformed space, SVR seeks to find a hyperplane that best fits the data. Unlike traditional regression that minimizes the residual sum of squares between observed and predicted values, SVR focuses on ensuring that errors do not exceed a specified threshold, the ε-insensitive tube. This approach allows some errors as long as they are within a certain margin, which is crucial for managing the noise inherent in complex datasets (Bui et al.; Marjanović et al., 2011; Tehrany et al., 2014). The objective of SVR is to find the flattest hyperplane in the feature space that fits the data. This hyperplane is determined by support vectors, which are data points that lie closest to the decision surface, or the boundary of the ε-insensitive tube. Maximizing the margin around this hyperplane allows SVR to achieve robust generalization, which is especially valuable in environmental modeling where outliers or unusual data points can disproportionately influence model performance (Marjanović et al., 2011). One of the key strengths of SVR is its use of kernel functions, which allow it to operate in a high-dimensional space without explicitly computing the coordinates of the data in that space. This feature as other ML method is crucial for handling complex, nonlinear relationships that are typical in hydrological data. The detailed explanation and mathematical formulation of SVR algorithm can be found Marjanović et al. (2011).

Appendix B

Table B.1. Statistical result of WRA modeling based on SVR, XGB, and RF for various independent variables combination

	No Var	R^2	RMSE	Var 1	Var 2	Var 3	Var 4	Var 5	Var 6	Var 7	Var 8
SVR	8	0.54	1.27	TRAV	RIP	RAD	RAMI	NRPO	RH	AT	WS
	7	0.59	1.19	TRAV	RIP	RAD	RAMI	NRPO	RH	AT	
	6	0.65	1.11	TRAV	RIP	RAD	RAMI	NRPO	AT		
	5	0.68	1.06	TRAV	RAD	RAMI	NRPO	AT			

	4	0.69	1.04	TRAV	RAD	NRPO	AT			
	3	0.72	0.98	TRAV	NRPO	RH				
	2	0.75	0.93	TRAV	NRPO					
	1	0.75	0.93	TRAV	NRPO					
XGB	8	0.76	0.91	TRAV	RIP	RAD	RAMI	NRPO	RH	AT	WS
	7	0.78	0.87	TRAV	RIP	RAD	RAMI	NRPO	RH	WS	
	6	0.78	0.87	TRAV	RIP	RAD	RAMI	NRPO	RH	WS	
	5	0.79	0.86	TRAV	RAD	RAMI	NRPO	WS			
	4	0.79	0.86	TRAV	RAD	RAMI	NRPO	WS			
	3	0.79	0.86	TRAV	RAD	RAMI	NRPO	WS			
	2	0.79	0.86	TRAV	NRPO						
	1	0.79	0.86	TRAV	NRPO						
RF	8	0.75	0.92	TRAV	RIP	RAD	RAMI	NRPO	RH	AT	WS
	7	0.79	0.85	TRAV	RIP	RAD	RAMI	NRPO	RH	AT	
	6	0.80	0.84	TRAV	RIP	RAD	NRPO	RH	AT		
	5	0.81	0.82	TRAV	RAD	RAMI	NRPO	AT			
	4	0.81	0.81	TRAV	RIP	NRPO	AT				
	3	0.81	0.81	TRAV	RIP	NRPO	AT				
	2	0.81	0.81	TRAV	RIP	NRPO	AT				
	1	0.81	0.81	TRAV	RIP	NRPO	AT				

Table B.2. Statistical result of TRUV modeling based on SVR, XGB, and RF for various independent variables combination

	No Var	R^2	RMSE	Var 1	Var 2	Var 3	Var 4	Var 5	Var 6	Var 7	Var 8
SVR	8	0.52	1.83	TRAV	RIP	RAD	RAMI	NRPO	RH	AT	WS
	7	0.55	1.78	TRAV	RIP	RAD	RAMI	RH	AT	WS	
	6	0.56	1.75	TRAV	RIP	RAD	RAMI	AT	WS		
	5	0.59	1.70	TRAV	RIP	RAD	RAMI	AT			
	4	0.62	1.63	TRAV	RIP	RAD	RAMI				
	3	0.65	1.58	TRAV	NRPO	RH					
	2	0.67	1.51	TRAV	RIP						
	1	0.67	1.51	TRAV	RIP						
XGB	8	0.71	1.42	TRAV	RIP	RAD	RAMI	NRPO	RH	AT	WS
	7	0.76	1.30	TRAV	RAD	RAMI	NRPO	RH	AT	WS	
	6	0.77	1.28	TRAV	RAD	NRPO	RH	AT	WS		
	5	0.77	1.27	TRAV	RAD	RAMI	NRPO	WS			
	4	0.77	1.27	TRAV	RAD	RAMI	NRPO	WS			

	3	0.77	1.27	TRAV	RAD	RAMI	NRPO	WS
	2	0.77	1.27	TRAV	RAD	RAMI	NRPO	WS
	1	0.77	1.27	TRAV	RAD	RAMI	NRPO	WS

RF	8	0.71	1.42	TRAV	RIP	RAD	RAMI	NRPO	RH	AT	WS
	7	0.73	1.38	TRAV	RAD	RAMI	NRPO	RH	AT	WS	
	6	0.75	1.34	TRAV	RIP	NRPO	RH	AT	WS		
	5	0.75	1.34	TRAV	RIP	NRPO	RH	AT	WS		
	4	0.75	1.31	TRAV	NRPO	RH	AT				
	3	0.76	1.30	TRAV	NRPO	AT					
	2	0.76	1.30	TRAV	NRPO						
	1	0.76	1.30	TRAV	NRPO						

Table B.3. Statistical result of TRD modeling based on SVR, XGB, and RF for various independent variables combination

	No Var	R^2	RMSE	Var 1	Var 2	Var 3	Var 4	Var 5	Var 6	Var 7	Var 8
SVR	8	0.44	2.59	TRAV	RIP	RAD	RAMI	NRPO	RH	AT	WS
	7	0.49	2.48	TRAV	RIP	RAD	RAMI	NRPO	RH	AT	
	6	0.53	2.37	TRAV	RIP	RAD	RAMI	RH	AT		
	5	0.56	2.29	TRAV	RIP	RAD	RAMI	AT			
	4	0.56	2.29	TRAV	RIP	RAD	AT				
	3	0.56	2.29	TRAV	RIP	RAD	AT				
	2	0.56	2.29	TRAV	RIP	RAD	AT				
	1	0.56	2.29	TRAV	RIP	RAD	AT				

XGB	8	0.60	2.19	TRAV	RIP	RAD	RAMI	NRPO	RH	AT	WS
	7	0.61	2.15	TRAV	RIP	RAD	NRPO	RH	AT	WS	
	6	0.63	2.11	TRAV	RIP	RAD	NRPO	RH	AT		
	5	0.64	2.06	TRAV	RIP	RAD	RAMI	NRPO			
	4	0.64	2.06	TRAV	RIP	RAD	RAMI	NRPO			
	3	0.64	2.06	TRAV	RIP	RAD	RAMI	NRPO			
	2	0.64	2.06	TRAV	RIP	RAD	RAMI	NRPO			
	1	0.64	2.06	TRAV	RIP	RAD	RAMI	NRPO			

RF	8	0.64	2.08	TRAV	RIP	RAD	RAMI	NRPO	RH	AT	WS
	7	0.67	1.99	TRAV	RIP	RAD	RAMI	NRPO	AT	WS	
	6	0.67	1.98	TRAV	RIP	RAD	RAMI	NRPO	AT		
	5	0.69	1.93	TRAV	RIP	RAD	NRPO	AT			
	4	0.69	1.93	TRAV	RIP	RAD	NRPO	AT			
	3	0.69	1.93	TRAV	RIP	RAD	NRPO	AT			

	2	0.69	1.93	TRAV	RIP	RAD	NRPO	AT
	1	0.69	1.93	TRAV	RIP	RAD	NRPO	AT

Table B.4. Statistical result of RUPFM modeling based on SVR, XGB, and RF for various independent variables combination

	No Var	R^2	RMSE	Var 1	Var 2	Var 3	Var 4	Var 5	Var 6	Var 7	Var 8
SVR	8	0.69	0.48	TRAV	RIP	RAD	RAMI	NRPO	RH	AT	WS
	7	0.74	0.45	TRAV	RIP	RAD	RAMI	NRPO	RH	AT	
	6	0.77	0.42	TRAV	RIP	RAD	RAMI	NRPO	RH		
	5	0.79	0.40	TRAV	RIP	RAMI	NRPO	RH			
	4	0.82	0.37	TRAV	RIP	NRPO	RH				
	3	0.82	0.37	TRAV	RIP	RAD					
	2	0.82	0.37	RIP	RH						
	1	0.82	0.37	RIP	RH						
XGB	8	0.77	0.42	TRAV	RIP	RAD	RAMI	NRPO	RH	AT	WS
	7	0.80	0.39	TRAV	RIP	RAD	NRPO	RH	AT	WS	
	6	0.81	0.38	TRAV	RIP	RAD	NRPO	RH	AT		
	5	0.82	0.37	RIP	RAD	RH	AT	WS			
	4	0.84	0.35	RIP	RAD	RH	AT				
	3	0.84	0.35	RIP	RAD	RH	AT				
	2	0.84	0.35	RIP	NRPO						
	1	0.84	0.35	RIP							
RF	8	0.82	0.37	TRAV	RIP	RAD	RAMI	NRPO	RH	AT	WS
	7	0.84	0.35	TRAV	RIP	RAD	RAMI	NRPO	RH	AT	
	6	0.84	0.35	TRAV	RIP	RAD	RAMI	RH	AT		
	5	0.84	0.34	RIP	RAD	RAMI	NRPO	AT			
	4	0.84	0.34	RIP	RAD	RAMI	NRPO	AT			
	3	0.84	0.34	RIP	RAD	RAMI	NRPO	AT			
	2	0.84	0.34	RIP	RAD	RAMI	NRPO	AT			
	1	0.84	0.34	RIP	RAD	RAMI	NRPO	AT			

Table B.5. Statistical result of PFR modeling based on SVR, XGB, and RF for various independent variables combination

	No Var	R^2	RMSE	Var 1	Var 2	Var 3	Var 4	Var 5	Var 6	Var 7	Var 8
SVR	8	0.28	0.60	TRAV	RIP	RAD	RAMI	NRPO	RH	AT	WS
	7	0.37	0.56	TRAV	RIP	RAD	RAMI	NRPO	AT	WS	
	6	0.44	0.53	TRAV	RIP	RAD	RAMI	NRPO	AT		

	5	0.49	0.51	TRAV	RIP	RAD	RAMI	NRPO
	4	0.59	0.45	RIP	RAD	NRPO	AT	
	3	0.70	0.39	RIP	RAD	NRPO		
	2	0.73	0.37	RIP	NRPO			
	1	0.73	0.37	RIP	NRPO			

XGB	8	0.55	0.47	TRAV	RIP	RAD	RAMI	NRPO	RH	AT	WS
	7	0.80	0.31	RIP	RAD	RAMI	NRPO	RH	AT	WS	
	6	0.81	0.31	RIP	RAD	RAMI	NRPO	RH	AT		
	5	0.82	0.30	RIP	RAMI	NRPO	RH	AT			
	4	0.82	0.30	RIP	NRPO	AT	WS				
	3	0.84	0.28	RIP	NRPO	WS					
	2	0.84	0.28	RIP	NRPO	WS					
	1	0.84	0.28	RIP	NRPO	WS					

RF	8	0.75	0.36	TRAV	RIP	RAD	RAMI	NRPO	RH	AT	WS
	7	0.77	0.34	RIP	RAD	RAMI	NRPO	RH	AT	WS	
	6	0.78	0.33	RIP	RAD	RAMI	NRPO	RH	WS		
	5	0.80	0.32	RIP	RAMI	NRPO	AT	WS			
	4	0.80	0.31	RIP	RAMI	NRPO	AT				
	3	0.81	0.31	RIP	RAMI	NRPO					
	2	0.81	0.31	RIP	RAD						
	1	0.81	0.31	RIP	RAD						

References

Adnan, R. M., Petroselli, A., Heddam, S., Santos, C. A. G., & Kisi, O. (2021). Comparison of different methodologies for rainfall–runoff modeling: machine learning vs conceptual approach. *Natural Hazards*, *105*(3), 2987-3011. https://doi.org/10.1007/s11069-020-04438-2

Basu, A. S., Basu, B., Pilla, F., & Sannigrahi, S. (2022). Investigating the performance of Green Roof for effective runoff reduction corresponding to different weather patterns: A case study in Dublin, Ireland. *Hydrology*, *9*(3), 46.

Basu, A. S., Pilla, F., Sannigrahi, S., Gengembre, R., Guilland, A., & Basu, B. (2021). Theoretical Framework to Assess Green Roof Performance in Mitigating Urban Flooding as a Potential Nature-Based Solution. *Sustainability*, *13*(23), 13231.

Bayat-Afshary, N., & Danesh-Yazdi, M. (2023). Are the magnitude and frequency of floods increasing in Iran due to climate change? Implications from a 50-year analysis. *Hydrological Sciences Journal*, *68*(15), 2243-2261.

Behzad, M., Asghari, K., Eazi, M., & Palhang, M. (2009). Generalization performance of support vector machines and neural networks in runoff modeling. *Expert Systems with applications*, *36*(4), 7624-7629.

Belgiu, M., & Drăguţ, L. (2016). Random forest in remote sensing: A review of applications and future directions. *ISPRS journal of photogrammetry and remote sensing*, *114*, 24-31.

Bhatta, B. (2010). Causes and consequences of urban growth and sprawl. In *Analysis of urban growth and sprawl from remote sensing data* (pp. 17-36). Springer.

Brandão, C., do Rosário Cameira, M., Valente, F., de Carvalho, R. C., & Paço, T. A. (2017). Wet season hydrological performance of green roofs using native species under Mediterranean climate. *Ecological Engineering*, *102*, 596-611.

Breiman, L. (2001). Random Forests. *Machine Learning*, *45*(1), 5-32. https://doi.org/10.1023/A:1010933404324

Bui, D., Pradhan, B., & Lofman, O. Revhaug. I., 2012. Landslide susceptibility assessment in vietnam using support vector machines, decision tree, and Naive Bayes Models. *Mathematical Problems in Engineering*, *2012*.

Butler, C., Butler, E., & Orians, C. M. (2012). Native plant enthusiasm reaches new heights: Perceptions, evidence, and the future of green roofs. *Urban forestry & urban greening*, *11*(1), 1-10.

Chen, C., & Pang, Y. (2019, 4-9 April 2019). Exploring Machine Learning Techniques for Smart Drainage System. 2019 IEEE Fifth International Conference on Big Data Computing Service and Applications (BigDataService),

Chen, J., Shi, X., Gu, L., Wu, G., Su, T., Wang, H.-M., Kim, J.-S., Zhang, L., & Xiong, L. (2023). Impacts of climate warming on global floods and their implication to current flood defense standards. *Journal of Hydrology*, *618*, 129236.

Chen, T., & Guestrin, C. (2016). Xgboost: A scalable tree boosting system. Proceedings of the 22nd acm sigkdd international conference on knowledge discovery and data mining,

Chen, T., He, T., Benesty, M., Khotilovich, V., Tang, Y., Cho, H., Chen, K., Mitchell, R., Cano, I., & Zhou, T. (2015). Xgboost: extreme gradient boosting. *R package version 0.4-2*, *1*(4), 1-4.

Cherkassky, V., & Mulier, F. M. (2007). *Learning from data: concepts, theory, and methods*. John Wiley & Sons.

Cohen-Shacham, E., Walters, G., Janzen, C., & Maginnis, S. (2016). Nature-based solutions to address global societal challenges. IUCN International Union for Conservation of Nature. In.

Dinh, T. L. A., & Aires, F. (2022). Nested leave-two-out cross-validation for the optimal crop yield model selection. *Geosci. Model Dev.*, *15*(9), 3519-3535. https://doi.org/10.5194/gmd-15-3519-2022

Feyen, L., Barredo, J., & Dankers, R. (2008). Implications of global warming and urban land use change on flooding in Europe. *Water and urban development paradigms–Towards an integration of engineering, design and management approaches*, 217-225.

Firozjaei, M. K., Kiavarz, M., Alavipanah, S. K., Lakes, T., & Qureshi, S. (2018). Monitoring and forecasting heat island intensity through multi-temporal image analysis and cellular automata-Markov chain modelling: A case of Babol city, Iran. *Ecological Indicators*, *91*, 155-170.

Firozjaei, M. K., Sedighi, A., Argany, M., Jelokhani-Niaraki, M., & Arsanjani, J. J. (2019). A geographical direction-based approach for capturing the local variation of urban expansion in the application of CA-Markov model. *Cities*, *93*, 120-135.

Firozjaei, M. K., Weng, Q., Zhao, C., Kiavarz, M., Lu, L., & Alavipanah, S. K. (2020). Surface anthropogenic heat islands in six megacities: An assessment based on a triple-source surface energy balance model. *Remote Sensing of Environment*, *242*, 111751.

Friedman, J. H. (2001). Greedy function approximation: a gradient boosting machine. *Annals of statistics*, 1189-1232.

Fu, Y., Li, J., Weng, Q., Zheng, Q., Li, L., Dai, S., & Guo, B. (2019). Characterizing the spatial pattern of annual urban growth by using time series Landsat imagery. *Science of The Total Environment*, *666*, 274-284.

Furtak, K., & Wolińska, A. (2023). The impact of extreme weather events as a consequence of climate change on the soil moisture and on the quality of the soil environment and agriculture–A review. *Catena*, *231*, 107378.

Getter, K. L., & Rowe, D. B. (2006). The role of extensive green roofs in sustainable development. *HortScience*, *41*(5), 1276-1285.

Getter, K. L., & Rowe, D. B. (2009). Substrate depth influences Sedum plant community on a green roof. *HortScience*, *44*(2), 401-407.

Graceson, A., Hare, M., Monaghan, J., & Hall, N. (2013). The water retention capabilities of growing media for green roofs. *Ecological Engineering*, *61*, 328-334.

Guo, Y., Zhang, Y., Zhang, L., & Wang, Z. (2021). Regionalization of hydrological modeling for predicting streamflow in ungauged catchments: A comprehensive review. *Wiley Interdisciplinary Reviews: Water*, *8*(1), e1487.

Hakimdavar, R., Culligan, P. J., Finazzi, M., Barontini, S., & Ranzi, R. (2014). Scale dynamics of extensive green roofs: Quantifying the effect of drainage area and rainfall characteristics on observed and modeled green roof hydrologic performance. *Ecological Engineering*, *73*, 494-508.

Huong, H. T. L., & Pathirana, A. (2013). Urbanization and climate change impacts on future urban flooding in Can Tho city, Vietnam. *Hydrology and Earth System Sciences*, *17*(1), 379-394.

Keck, T. (2016). Fastbdt: A speed-optimized and cache-friendly implementation of stochastic gradient-boosted decision trees for multivariate classification. arXiv: 160906119. *arXiv preprint arXiv:1609.06119*.

Kemp, S., Hadley, P., & Blanuša, T. (2019). The influence of plant type on green roof rainfall retention. *Urban Ecosystems*, *22*, 355-366.

Le, L., Nguyen, H., Jian, Z., & Dou, J. (2019). Estimating the heating load of energy efficiency of buildings for smart city planning using a novel artificial intelligence technique PSO-XGBoost. *Appl Sci*.

Lhomme, S., Laganier, R., Diab, Y., & Serre, D. (2019). The resilience of the city of Dublin to flooding: From theory to practice. *Cybergeo: European Journal of Geography*.

Li, J., Li, D., Xiong, C., & Hoi, S. (2022). Blip: Bootstrapping language-image pre-training for unified vision-language understanding and generation. International conference on machine learning,

Li, X., Cao, J., Xu, P., Fei, L., Dong, Q., & Wang, Z. (2018). Green roofs: Effects of plant species used on runoff. *Land Degradation & Development*, *29*(10), 3628-3638.

Li, X., Sha, J., & Wang, Z.-L. (2019). Comparison of daily streamflow forecasts using extreme learning machines and the random forest method. *Hydrological Sciences Journal*, *64*(15), 1857-1866.

Li, Y., Gou, J., & Fan, Z. (2019, 20-22 Dec. 2019). Particle swarm optimization-based extreme gradient boosting for concrete strength prediction. 2019 IEEE 4th Advanced Information Technology, Electronic and Automation Control Conference (IAEAC),

Liu, W., Feng, Q., Chen, W., Wei, W., & Deo, R. C. (2019). The influence of structural factors on stormwater runoff retention of extensive green roofs: new evidence from scale-based models and real experiments. *Journal of Hydrology*, *569*, 230-238.

Man, C. D., Nguyen, T. T., Bui, H. Q., Lasko, K., & Nguyen, T. N. T. (2018). Improvement of land-cover classification over frequently cloud-covered areas using Landsat 8 time-series composites and an ensemble of supervised classifiers. *International Journal of Remote Sensing*, *39*(4), 1243-1255.

Marjanović, M., Kovačević, M., Bajat, B., & Voženílek, V. (2011). Landslide susceptibility assessment using SVM machine learning algorithm. *Engineering Geology*, *123*(3), 225-234.

Mentens, J., Raes, D., & Hermy, M. (2006). Green roofs as a tool for solving the rainwater runoff problem in the urbanized 21st century? *Landscape and urban planning*, *77*(3), 217-226.

Metselaar, K. (2012). Water retention and evapotranspiration of green roofs and possible natural vegetation types. *Resources, conservation and recycling*, *64*, 49-55.

Micheletti, N., Foresti, L., Robert, S., Leuenberger, M., Pedrazzini, A., Jaboyedoff, M., & Kanevski, M. (2014). Machine learning feature selection methods for landslide susceptibility mapping. *Mathematical geosciences*, *46*, 33-57.

Mienye, I. D., & Sun, Y. (2022). A survey of ensemble learning: Concepts, algorithms, applications, and prospects. *IEEE Access*, *10*, 99129-99149.

Moguerza, J. M., & Muñoz, A. (2006). Support vector machines with applications.

Monterusso, M., Rowe, D., Rugh, C., & Russell, D. (2002). Runoff water quantity and quality from green roof systems. XXVI International Horticultural Congress: Expanding Roles for Horticulture in Improving Human Well-Being and Life Quality 639,

MORAN, A. C., HUNT, B., & JENNINGS, G. (2004). *A North Carolina field study to evaluate greenroof runoff quantity, runoff quality, and plant growth. 300f* Dissertação (Mestrado em Biological Agricultural Engineering)–Graduate …].

Morgan, S., Celik, S., & Retzlaff, W. (2013). Green roof storm-water runoff quantity and quality. *Journal of Environmental Engineering*, *139*(4), 471-478.

Mountrakis, G., Im, J., & Ogole, C. (2011). Support vector machines in remote sensing: A review. *ISPRS journal of photogrammetry and remote sensing*, *66*(3), 247-259. https://doi.org/https://doi.org/10.1016/j.isprsjprs.2010.11.001

Mukonza, S. S., & Chiang, J. L. (2022, 7-9 March 2022). Quantifying Cross-Validation Uncertainties for Linear Regression Machine Learning Algorithm Used to Estimate Chlorophyll-a in Mundan Water Reservoir Based on Landsat Derived Spectral Indices. 2022 IEEE Mediterranean and Middle-East Geoscience and Remote Sensing Symposium (M2GARSS),

Nagase, A., & Dunnett, N. (2011). The relationship between percentage of organic matter in substrate and plant growth in extensive green roofs. *Landscape and urban planning*, *103*(2), 230-236.

Nawaz, R., McDonald, A., & Postoyko, S. (2015). Hydrological performance of a full-scale extensive green roof located in a temperate climate. *Ecological Engineering*, *82*, 66-80.

Nielsen, D. (2016). *Tree boosting with xgboost-why does xgboost win" every" machine learning competition?* NTNU].

OWUSU, A. B., MENSAH, C. A., BLAY, J., & FYNN, I. E. M. (2023). URBAN GROWTH AND LAND SURFACE TEMPERATURE DYNAMICS. *Theoretical and Empirical Researches in Urban Management*, *18*(3), 50-65.

Palermo, S. A., Turco, M., Principato, F., & Piro, P. (2019). Hydrological effectiveness of an extensive green roof in Mediterranean climate. *Water*, *11*(7), 1378.

Palla, A., Sansalone, J. J., Gnecco, I., & Lanza, L. G. (2011). Storm water infiltration in a monitored green roof for hydrologic restoration. *Water Science and Technology*, *64*(3), 766-773.

Pappas, E., Smith, D., Huang, C., Shuster, W., & Bonta, J. (2008). Impervious surface impacts to runoff and sediment discharge under laboratory rainfall simulation. *Catena*, *72*(1), 146-152.

Paranunzio, R., Guerrini, M., Dwyer, E., Alexander, P. J., & O'Dwyer, B. (2022). Assessing Coastal Flood Risk in a Changing Climate for Dublin, Ireland. *Journal of Marine Science and Engineering*, *10*(11), 1715.

Pilla, F., Gharbia, S. S., & Lyons, R. (2019). How do households perceive flood-risk? The impact of flooding on the cost of accommodation in Dublin, Ireland. *Science of The Total Environment*, *650*, 144-154.

Poë, S., Stovin, V., & Berretta, C. (2015). Parameters influencing the regeneration of a green roof's retention capacity via evapotranspiration. *Journal of Hydrology*, *523*, 356-367.

Pourghasemi, H. R., & Kerle, N. (2016). Random forests and evidential belief function-based landslide susceptibility assessment in Western Mazandaran Province, Iran. *Environmental earth sciences*, *75*, 1-17.

Qin, Y. (2020). Urban flooding mitigation techniques: A systematic review and future studies. *Water*, *12*(12), 3579.

Rahmani, F., & Fattahi, M. H. (2024). Investigation of alterations in droughts and floods patterns induced by climate change. *Acta Geophysica*, *72*(1), 405-418.

Rennie, J. D. (2003). On the value of leave-one-out cross-validation bounds. *Computers in Biology and Medicine*, 123-129.

Roehr, D., & Kong, Y. (2010). Runoff reduction effects of green roofs in Vancouver, BC, Kelowna, BC, and Shanghai, PR China. *Canadian Water Resources Journal*, *35*(1), 53-68.

Sagi, O., & Rokach, L. (2018). Ensemble learning: A survey. *Wiley interdisciplinary reviews: data mining and knowledge discovery*, *8*(4), e1249.

Schreider, S. Y., Smith, D., & Jakeman, A. (2000). Climate change impacts on urban flooding. *Climatic Change*, *47*, 91-115.

Shafique, M., Kim, R., & Kyung-Ho, K. (2018). Rainfall runoff mitigation by retrofitted permeable pavement in an urban area. *Sustainability*, *10*(4), 1231.

Shuster, W. D., Bonta, J., Thurston, H., Warnemuende, E., & Smith, D. (2005). Impacts of impervious surface on watershed hydrology: A review. *Urban Water Journal*, *2*(4), 263-275.

Snodgrass, E. C., & Snodgrass, L. L. (2006). *Green roof plants: a resource and planting guide* (Vol. 480). Timber Press Portland, OR.

Solomon, D. D., Khan, S., Garg, S., Gupta, G., Almjally, A., Alabduallah, B. I., Alsagri, H. S., Ibrahim, M. M., & Abdallah, A. M. A. (2023). Hybrid Majority Voting: Prediction and Classification Model for Obesity. *Diagnostics*, *13*(15), 2610. https://www.mdpi.com/2075-4418/13/15/2610

Soulis, K., & Valiantzas, J. (2012). Variation of runoff curve number with rainfall in heterogeneous watersheds. The Two-CN system approach. *Hydrology and Earth System Sciences*, *16*(3), 1001-1015.

Soulis, K. X., Ntoulas, N., Nektarios, P. A., & Kargas, G. (2017). Runoff reduction from extensive green roofs having different substrate depth and plant cover. *Ecological Engineering*, *102*, 80-89.

Speak, A., Rothwell, J., Lindley, S., & Smith, C. (2013). Rainwater runoff retention on an aged intensive green roof. *Science of The Total Environment*, *461*, 28-38.

Sreedharan, R., Prajapati, J., Engineer, P., & Prajapati, D. (2023). 5 Leave-One-Out Validation in Machine Cross-Learning. *Ethical Issues in AI for Bioinformatics and Chemoinformatics*, 56.

Stovin, V. (2010). The potential of green roofs to manage urban stormwater. *Water and Environment Journal*, *24*(3), 192-199.

Stovin, V., Poë, S., & Berretta, C. (2013). A modelling study of long term green roof retention performance. *Journal of environmental management*, *131*, 206-215.

Stovin, V., Poë, S., De-Ville, S., & Berretta, C. (2015). The influence of substrate and vegetation configuration on green roof hydrological performance. *Ecological Engineering*, *85*, 159-172.

Stovin, V., Vesuviano, G., & Kasmin, H. (2012). The hydrological performance of a green roof test bed under UK climatic conditions. *Journal of Hydrology*, *414*, 148-161.

Tamm, O., Saaremäe, E., Rahkema, K., Jaagus, J., & Tamm, T. (2023). The intensification of short-duration rainfall extremes due to climate change–Need for a frequent update of intensity–duration–frequency curves. *Climate Services*, *30*, 100349.

Tehrany, M. S., Pradhan, B., & Jebur, M. N. (2014). Flood susceptibility mapping using a novel ensemble weights-of-evidence and support vector machine models in GIS. *Journal of Hydrology*, *512*, 332-343.

VanWoert, N. D., Rowe, D. B., Andresen, J. A., Rugh, C. L., Fernandez, R. T., & Xiao, L. (2005). Green roof stormwater retention: effects of roof surface, slope, and media depth. *Journal of environmental quality*, *34*(3), 1036-1044.

Vapnik, V. N., & Vapnik, V. (1998). Statistical learning theory.

Wan, S., & Lei, T. C. (2009). A knowledge-based decision support system to analyze the debris-flow problems at Chen-Yu-Lan River, Taiwan. *Knowledge-Based Systems*, *22*(8), 580-588.

Wong, G. K., & Jim, C. Y. (2014). Quantitative hydrologic performance of extensive green roof under humid-tropical rainfall regime. *Ecological Engineering*, *70*, 366-378.

Wu, S., Bates, B., Zbigniew Kundzewicz, A., & Palutikof, J. (2008). Climate change and water. *Technical Paper of the Intergovernmental Panel on Climate Change. Geneva*.

Xiang, Y., Chen, J., Li, L., Peng, T., & Yin, Z. (2021). Evaluation of eight global precipitation datasets in hydrological modeling. *Remote Sensing*, *13*(14), 2831.

Xu, C., Rahman, M., Haase, D., Wu, Y., Su, M., & Pauleit, S. (2020). Surface runoff in urban areas: The role of residential cover and urban growth form. *Journal of Cleaner Production*, *262*, 121421.

Yang, W.-Y., Li, D., Sun, T., & Ni, G.-H. (2015). Saturation-excess and infiltration-excess runoff on green roofs. *Ecological Engineering*, *74*, 327-336.

Yang, Y., & Chui, T. F. M. (2021). Modeling and interpreting hydrological responses of sustainable urban drainage systems with explainable machine learning methods. *Hydrology and Earth System Sciences*, *25*(11), 5839-5858.

Yao, X., Tham, L., & Dai, F. (2008). Landslide susceptibility mapping based on support vector machine: a case study on natural slopes of Hong Kong, China. *Geomorphology*, *101*(4), 572-582.

Zhu, H., Yu, M., Zhu, J., Lu, H., & Cao, R. (2019). Simulation study on effect of permeable pavement on reducing flood risk of urban runoff. *International journal of transportation science and technology*, *8*(4), 373-382.